INVESTIGATING PATERA GEOMORPHOLOGY IN NORTHWEST ARABIA, MARS WITH SHARAD RADARGRAMS. S. Culvahouse[1], J. L. Whitten[2], N. Abu Hashmeh[3], and S. Karunatillake[4], [1]Tulane University (sculvahouse@tulane.edu), [2]Tulane University (jwhitten1@tulane.edu), [3]Tulane University (nabuhashmeh@tulane.edu), [4]Geology & Geophysics, Louisiana State University (sunitiw@lsu.edu).

Introduction: Michalski and Bleacher first proposed super-eruptions in NW Arabia Terra [1], with subsequent reinforcing interpretations [2, 3]. However, the associated climate-transforming extent of eruptive units and the underlying state of the Martian interior remain poorly known [4]. Those observations collectively motivate our work to identify volcanic strata in the patera landscape and to determine their origin and composition. The dominating presence of surface-lateral reflectors inhibit analysis of subsurface contacts, but ultimately proved useful as a proxy for comparing geomorphology of the proposed patera with other types of features, such as impact craters of similar size and age.

Fig. 1: Context map highlighting target features (paterae and impact craters used as alternative references). Blue lines indicate SHARAD tracks used for analysis.

Methods: SHARAD (Shallow Radar, instrument aboard the Mars Reconnaissance Orbiter) tracks were selected using the JMARS application [5] to identify product IDs for tracks running through center (or as close to center as possible) of proposed paterae (Eden, Euphrates, Ismenia, Oxus, Siloe) and key alternative references such as Medusa Fossae Formation, Bamberg Crater, and Focas Crater. Once SHARAD product IDs were determined, the radargram portable network graphics (PNGs) were retrieved from Mars Image Explorer [6]. A clutter simulation was then run for each of the chosen tracks using the CO-SHARPS (Colorado SHARAD Radar Processing System) processing boutique [7], a tool which simulates radargrams using MOLA (Mars Orbiter Laser Altimeter, instrument aboard the Mars Global Surveyor) topography data. From the CO-SHARPS output, the echo map (MOLA topography image with markers indicating the location of off-nadir surface reflections) and simulated radargram files were saved for each track. A Mathematica program was used to subtract the clutter simulations from the radargram images which isolated data in the radargrams that actually represent subsurface contacts, rather than off-nadir surface lateral reflections (clutter) (Fig. 2). An additional Mathematica program calculated surface-lateral reflector distances (from nadir track) from the echo map images. These distances were then used to create a cumulative distribution function plot showing the distribution of surface-lateral reflector distances for the different target features.

Results:

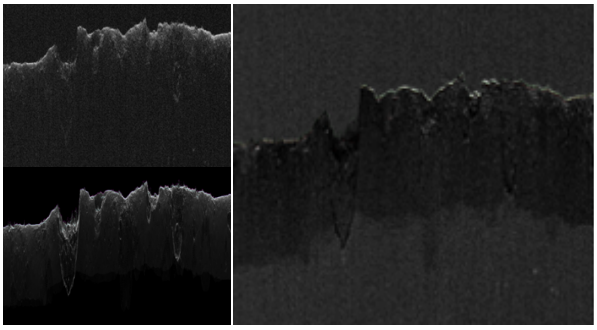

Track ID: S_06681201

Fig. 2: Subset of a SHARAD radargram of Ismenia Patera. Right image is generated by subtracting a clutter-simulation (lower left) from a PDS radargram (upper left). (Brightness of right image increased by 30% to enhance visibility.)

Post-subtraction, most of the subsurface reflectors disappear, indicating that most of the reflectors recorded in the radargram are from off-nadir topographic features rather than subsurface stratigraphic contacts (Fig. 2). A few reflectors remain in the post-subtraction image but cross referencing with the clutter simulation confirms that these are also surface lateral reflections.

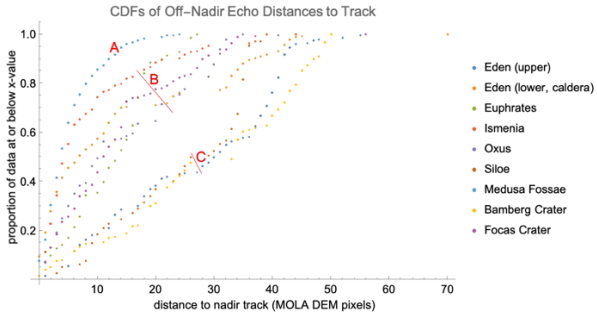

Fig. 3: Cumulative distribution function plot showing distances from off-nadir surface reflectors to SHARAD nadir-track. Three groups emerge, labeled A, B and C.

Two main trends emerge from the CDF plot, though the proposed super-volcanic patera appear in both groups. Group B in Fig. 3 (Ismenia, Euphrates, Eden [lower basin], and Oxus Paterae, and Focas Crater) is

defined by features with a greater proportion of short off-nadir reflector distances. Group C in Fig. 3 (Siloe Patera, Eden Patera [upper basin], and Bamberg Crater) is defined by features with a greater proportion of long off-nadir reflector distances. A third trend could be argued, Group A in Fig. 3, represented by the Medusa Fossae Formation, which defines an upper boundary on the plot; though also defined by short off-nadir reflector distances, this plot appears somewhat separated from the rest of group B.

Discussion: Though the CDF plot for surface lateral reflector distances showed some defined trends, there was not a clear trend for all of the proposed patera vs. other target features. Rather, patera appeared in both groups. This occurrence could be explained by the diameter of the patera or surface roughness within the patera basin. For example, from a visual analysis Ismenia Patera appears to have a high terrain roughness, and its radargrams were dominated by shorter off-nadir reflector distances (Figs. 3, 4). This texture could result from an eruption dominated by blocky pyroclastic material of poorly sorted heterogenous granulometry, rather than the smoother surface produced by an effusive eruption.

The Medusa Fossae Formation (MFF) is also dominated by shorter off-nadir reflector distances. The lack of a rim feature at the MFF could account for this, as the radar signal may not immediately interact with and be reflected back by an outstanding feature at a further distance from the nadir track. The echo map images (Fig. 4) make clear that the rim features of the patera (as well as the impact craters) play a role in the number, and distance from nadir, of surface lateral reflectors.

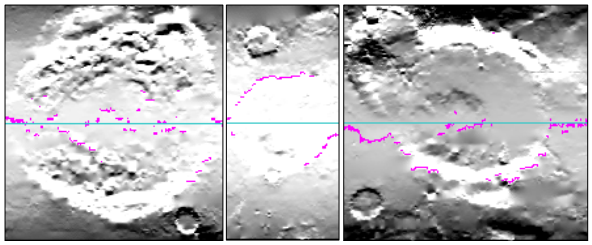

Track IDs: S_06681201, S_04984001, S_03799901

Fig. 4: CO-SHARPS echo maps of (left to right) Ismenia, Siloe, and Eden Paterae. Clutter from off-nadir surface reflectors (pink pixels) comes mainly from interior topographic features for Ismenia Patera, whereas clutter comes mainly from rim features for Siloe and Eden Paterae.

Impact craters with diameters much larger than those included in the CDF plot did not return as many surface-lateral reflectors from the rim as it was too far from the track running through the center of the basin. Ultimately there appeared to be a size range, which the proposed patera fall into, in which the surface lateral reflectors picked up the rim features, elevating apparent subsurface data.

The high ratio of surface lateral reflections to actual subsurface reflections in radargrams of the proposed paterae could be explained a couple of ways. First, as discussed above, the nature of the eruptive event created a large amount of surface texture that is then picked up by the instrument (in contrast with effusive volcanic features such as Elysium and Syrtis). A second, but related, explanation could be that if the eruptive event was dominated by heterogeneous pyroclastics, the buried ejecta may not be consistently–or contiguously–stratified enough to create a distinct contact layer in radargrams. Clasts may not follow a granulometric gradient, particularly in an exceptionally energetic eruption, to form stratified layers. Thirdly, if the eruptive event was dominated by low density or high surface area/mass volcanic ash, much of the ejected material may have deposited distally from the eruptive site, and is thus absent in locally targeted radargrams.

Conclusion and Future Work: Though the radargram analysis did not reveal unambiguous volcano-sedimentary strata within the subsurface of the proposed patera, analyzing surface lateral reflections recorded in the radargrams proved a promising method for identifying geomorphological trends for paterae, craters, and other features on Mars. Continuing with this project, more target features of different proposed origins, size, age, and location will be analyzed and compared with the current data. Another step that could be taken would be to investigate what factors lead to some surface lateral features being recorded by the radar instrument, while others are not. The simulated radargrams identify more surface lateral reflections than appear in the actual radargrams; rather than isolating the subsurface reflections, one could identify and investigate the surface lateral reflections which are recorded by the actual radargram in contrast with those suggested by the simulation.

Acknowledgements: NASA Summer Undergraduate Program for Planetary Research (Lunar and Planetary Institute, Universities Space Research Association), NASA Planetary Data System, CO-SHARPS, Dr. Stuart Robbins (Southwest Research Institute, Boulder), Augustus Bates (Louisiana State University), Natalie Lovegren (University of Texas Austin), LSU Planetary Science Laboratory.

References: **[1]** Michalski, J. and Bleacher, J. (2013) DOI: 10.1038/nature12482 **[2]** Whelley et al. (2021) DOI: 10.1029/2021GL094109 **[3]** Rani et al. (2021) *LPSC LII*, Abstract #2353. **[4]** Bates et al. (2020) *LPSC LI*, Abstract #1588. **[5]** JMARS: https://jmars.asu.edu/ **[6]** Mars Image Explorer: http://viewer.mars.asu.edu/viewer/sharad#T=0 **[7]** CO-SHARPS Processing Boutique: https://sharad.psi.edu/cosharps.php